for the antiferromagnetically exchange coupled $S = {}^1/_2$ ions with $J = -1.0$ (1) cm^{-1} and $g = 2.12$ (2). These results will now be examined in view of the magnetostructural correlations that are being developed.[27]

The ϕ/R_0 value for the Cu-Cl-Cu segment of the chain is 34.4° $Å^{-1}$. (The Cu-Cl-Cu angle is 95.6 (2)°, and the long Cu-Cl bond distance is 2.776 (6) Å.) This ϕ/R_0 value is intermediate between those found for bis(μ-chloro)-bridged and mono(μ-chloro)-bridged copper(II) chains.[27] A ϕ/R_0 value of 34.4 for a bis(μ-chloro)-bridged copper(II) dimer would lead to the prediction of a small negative exchange coupling constant for the Cu-Cl-Cu segment of the chain, as observed.

There are no nitrogen bridged chain precedents with which the ϕ/R_0 value for the Cu-N-Cu segment may be compared. On the basis of the Cu-N-Cu angle of 89.1°, a ferromagnetic exchange may be expected.

Conclusions. Three new compounds of the neutral ligand oxamide oxime have been prepared and characterized. The neutral ligand is involved in inter- and intramolecular hydrogen bonding, although the intermolecular hydrogen bonding in the monomeric compound $[Cu(oaoH_2)_2(H_2O)]SO_4$ does not lead to detectable exchange coupling. The new dimeric compound has bis(μ-sulfato) bridges, which are rare. This work demonstrates that the sulfate bridging ligand provides an effective pathway for superexchange interactions. The singlet-triplet splitting in $[Cu(oaoH_2)(H_2O)(SO_4)]_2$ is 2.55 cm^{-1}. It is anticipated that exchange coupling may be detected in the μ-sulfato-bridged chain compound $[Cu(oaoH_2)(H_2O)(SO_4)]_n$, however, it was not possible to prepare an adequate quantity of sample for magnetic susceptibility measurements. Magnetic susceptibility measurements revealed the presence of exchange coupling in $[Cu(oaoH_2)Cl_2]_\infty$, and once adequate data on similar compounds are available, it should be possible to determine from magnetostructural correlations whether the compound should be described as a mono(μ-chloro)-bridged copper(II) chain or a (μ-chloro,μ-nitrogen)-bridged chain.

Acknowledgment. This research was supported by the Fonds der Chemischen Industrie and the National Science Foundation through Grant No. CHE 83 08129.

Registry No. 1, 91743-23-6; 2, 91743-24-7; 3, 91743-26-9; $[Cu(oaoH_2)Cl_2]_n$, 91743-28-1.

Supplementary Material Available: Figures of magnetic susceptibility data for $[Cu(oaoH_2)_2(H_2O)]SO_4$ and $[Cu(oaoH_2)Cl_2]_n$ and listings of temperature factors and of calculated and observed structure amplitudes (27 pages). Ordering information is given on any current masthead page.

(28) Bonner, J. C.; Fisher, M. E. *Phys. Rev. A* **1964**, *135*, 640.
(29) Hatfield, W. E.; Weller, R. R.; Hall, J. W. *Inorg. Chem.* **1980**, *19*, 3825-3828.

Contribution from the Department of Natural Sciences, Baruch College, New York, New York 10010, and Department of Chemistry, Brookhaven National Laboratory, Upton, New York 11973

Electron-Transfer Barriers and Metal-Ligand Bonding as a Function of Metal Oxidation State. 3. Crystal and Molecular Structures of Tris(2,2'-bipyridine)nickel(III) Triperchlorate-2-Acetonitrile-0.5-Dichloromethane[1,3]

DAVID J. SZALDA,[2a,b] DONAL H. MACARTNEY,[2b] and NORMAN SUTIN*[2b]

Received January 20, 1984

The structure of tris(2,2'-bipyridine)nickel(III) triperchlorate-2-acetonitrile-0.5-dichloromethane, $[Ni(C_{10}H_8N_2)_3](ClO_4)_3 \cdot 2CH_3CN \cdot 0.5CH_2Cl_2$, has been determined. The nickel(III) complex crystallizes in the triclinic crystal system, space group $P\bar{1}$, with $a = 11.193$ (1) Å, $b = 17.634$ (3) Å, $c = 10.494$ (2) Å, $\alpha = 95.41$ (1)°, $\beta = 107.02$ (2)°, $\gamma = 95.28$ (1)°, and $Z = 2$. The structure was refined to a final R value of 0.096. The coordination sphere consists of the six nitrogen atoms of the three bipyridine ligands in a tetragonally distorted octahedral arrangement about the nickel. The six nickel-nitrogen bonds form three sets with two pairs of longer equatorial bonds, 2.022 (6) and 2.000 (5) Å, and a pair of shorter axial bonds, 1.924 (6) Å. The metal-ligand bond distances in $Ni(bpy)_3^{3+}$ and related complexes are rationalized in terms of their electronic configurations. The electron-transfer barrier for the $Ni(bpy)_3^{3+}$-$Ni(bpy)_3^{2+}$ exchange is related to the bond length differences in the two oxidation states and is compared with the barrier for electron transfer between other polypyridine complexes.

Introduction

Although a number of theories of electron-transfer reactions have been proposed, there is general agreement that the changes in nuclear configuration that occur when a molecule or ion is oxidized or reduced is an important factor in determining electron-transfer rates.[4] If the reactants are two metal complexes, then these configuration changes include changes in the metal-ligand and intraligand bond distances and angles, as well as changes in the orientations of the surrounding (polar) solvent molecules. The series of tris(bipyridine) (or tris(phenanthroline)) complexes provide excellent systems for testing these models, since, despite the formal similarity of the polypyridine couples, their measured exchange rates span 8 orders of magnitude.

In terms of a recent semiclassical model[4-6] the rate constant k for an electron-exchange reaction such as

$$M(bpy)_3^{2+} + M(bpy)_3^{3+} \rightleftharpoons M(bpy)_3^{3+} + M(bpy)_3^{2+} \quad (1)$$

may be expressed as the product of a preequilibrium constant K_A, an effective nuclear frequency ν_n, and electronic and nuclear factors κ_{el} and κ_n, respectively:

$$k = K_A \nu_n \kappa_{el} \kappa_n \quad (2)$$

The value of the preequilibrium constant depends upon the

(1) Part 2 in this series is ref 3.
(2) (a) Baruch College. (b) Brookhaven National Laboratory.
(3) Szalda, D. J.; Creutz, C.; Mahajan, D.; Sutin, N. *Inorg. Chem.* **1983**, *22*, 2372.
(4) Sutin, N. *Acc. Chem. Res.* **1982**, *15*, 275. Sutin, N. *Prog. Inorg. Chem.* **1983**, *30*, 441.
(5) Brunschwig, B. S.; Logan, J.; Newton, M. D.; Sutin, N. *J. Am. Chem. Soc.* **1980**, *102*, 5789.
(6) Brunschwig, B. S.; Creutz, C.; Macartney, D. H.; Sham, T. K.; Sutin, N. *Discuss. Faraday Soc.* **1982**, *74*, 113.

0020-1669/84/1323-3473$01.50/0

charges and sizes of the reactants; rate variations from this source are less than 1 order of magnitude for the tris(polypyridine) complexes in the media used.[4] Similarly, the product of the nuclear frequency and electronic factors is expected to vary by less than 2 orders of magnitude for the polypyridine systems.[4] On this basis the factor of 10^8 variation in the exchange rates of the tris(polypyridine) couples must arise primarily from changes in the nuclear factor. For exchange reactions the nuclear factor is given by eq 3, where Γ_λ is a

$$\kappa_n = \Gamma_\lambda \exp[-(\Delta G^*_{out} + \Delta G^*_{in})/RT] \quad (3)$$

nuclear tunneling factor and ΔG^*_{out} and ΔG^*_{in} are the solvent and inner-shell reorganization energies, respectively. Since ΔG^*_{out} depends only on the sizes of the complexes and on the properties of the solvent, it is essentially constant for the tris(polypyridine) couples in a given medium. Consequently, the 10^8 variation in the exchange rates of the polypyridine couples should largely reflect changes in ΔG^*_{in}.

A previous study has focused on the magnitude of ΔG^*_{in} for exchange reactions of tris(bipyridine)cobalt(III,II) and -(II,I) couples.[3] Here we report structural data for $Ni(bpy)_3^{3+}$ and correlate the $Ni(bpy)_3^{3+/2+}$ exchange rate with the structural changes accompanying the electron transfer. The $Ni(bpy)_3^{3+}$ ion is a very strong oxidant (1.72 V vs. NHE), and kinetic studies of its redox reactions (as well as those of other nickel(III) complexes[12,13]) have been reported.[7-11] The structural changes and redox reactivity of the $Ni(bpy)_3^{3+/2+}$ couple, in which the nickel(III) is low spin $[(\pi d)^6(\sigma d)^1]$ and the nickel(II) high spin $[(\pi d)^6(\sigma d)^2]$, afford an interesting comparison with the isoelectronic $Co(bpy)_3^{2+/+}$ couple, in which the two complexes are both high spin with $[(\pi d)^5(\sigma d)^2]$ and $[(\pi d)^6(\sigma d)^2]$ configurations, respectively.

Experimental Section

Preparation of $Ni(bpy)_3(ClO_4)_3 \cdot 2CH_3CN \cdot 0.5CH_2Cl_2$. The complex $Ni(bpy)_3(ClO_4)_2$ was prepared by the addition of 3.2 equiv of 2,2'-bipyridine (G. F. Smith) to 1.0 equiv of $Ni(ClO_4)_2 \cdot 6H_2O$ (G. F. Smith) in methanol. The pink precipitate was filtered, washed with methanol and ether, and vacuum dried. The nickel(III) complex was synthesized electrochemically[14] from $Ni(bpy)_3(ClO_4)_2$ in anhydrous CH_3CN containing 0.05 M tetrabutylammonium perchlorate. The solvent was removed by evaporation and the dark green solid washed with anhydrous CH_2Cl_2 to remove unreacted Ni(II) and the electrolyte. The crystals were grown by suspending a solution of $Ni(bpy)_3(ClO_4)_3$ in CH_3CN above an equal volume of CH_2Cl_2 in a stoppered test tube. After several days at 5 °C, dark green crystals formed. The crystals were washed with CH_2Cl_2 and stored in a desiccator at 5 °C in the dark. Anal. Calcd for $Ni(bpy)_3(ClO_4)_3 \cdot 2CH_3CN \cdot 0.5CH_2Cl_2$: Ni, 6.18. Found: Ni, 6.2. Far-infrared: ν(Ni–N) = 374 and 275 cm^{-1}. The far-infrared spectra were measured on a Perkin-Elmer 180 infrared spectrometer. Nujol mulls of solid samples were used with polyethylene plates.

Collection and Reduction of X-ray Data. Tris(2,2'-bipyridine)-nickel(III) Triperchlorate–2-Acetonitrile–0.5-Dichloromethane. This compound crystallizes as dark green prisms. Because of the instability of the crystals at room temperature, data were collected at low temperature by passing a stream of cooled N_2 around the crystal. Most of the crystals appeared to be twinned, but one recrystallization yielded several good crystals. These crystals showed $\bar{1}$ Laue symmetry and no systematic absences, consistent with the triclinic space groups $P1$ (No. 1, C_1^1)[15a] and $P\bar{1}$ (No. 2, C_i^1).[15b]

Data were collected on a 0.367 × 0.340 × 0.218 mm^3 crystal mounted on a glass fiber. The crystal was gradually cooled to 160 K, and the $\pm h \pm k l$ hemisphere of intensity data was collected. During data collection the intensities of the standard reflections underwent two increases of 3–8%: the intensities were relatively constant before these increases and remained constant thereafter. Despite these increases, the unit cell volume and constants did not change significantly during the data collection. (These increases may have been due to solid-state transitions involving the disordered solvent molecules.[16]) The data were scaled[17] to correct for these increases. Crystal data and details of the data collection and reduction are given in Table I.

Table I. Experimental Details of the X-ray Diffraction Study of $Ni(C_{10}H_8N_2)_3(ClO_4)_3 \cdot 2CH_3CN \cdot 0.5CH_2Cl_2$

(A) Crystal Parameters[a] at 160 K[b]	
a, Å	11.193 (1)
b, Å	17.634 (3)
c, Å	10.494 (2)
α, deg	95.41 (1)
β, deg	107.02 (1)
γ, deg	95.28 (1)
V, Å^3	1956.1
Z	2
mol wt	950.18
space group	$P\bar{1}$
ρ(exptl), g cm^{-3}	1.57
ρ(calcd), g cm^{-3} [c]	1.613 (160 K), 1.563 (296 K)
(B) Measurement of Intensity Data	
instrument	Enraf-Nonius CAD-4 diffractometer fitted with an Enraf-Nonius low-temperature device
radiation	Cu Kα (λ_{α_1} = 1.540 51 Å), graphite monochromatized
2θ limits, deg	2–140
scan type	θ(cryst)–2θ(counter)
stds	3 reflcns, $(22\bar{1})$, $(31\bar{1})$, and $(30\bar{1})$, measd after each 1 h of exposure time; these stds varied by 8–21% during data collection
(C) Treatment of Intensity Data[d]	
reduction to preliminary F_o and $\sigma(F_o)$	cor for bkgd, attenuators, and and Lorentz-polarization effects of monochromatized X radiation in the usual manner
abs cor[e]	μ = 35.9 cm^{-1} max and min; transmission coeff 0.5280 and 0.2904, respectively
obsd data	7599 reflcns collected, of which 5087 having $F_o > 5\sigma(F_o)$ used in refinement

[a] From a least-squares fit to the setting angles of 25 reflections with $2\theta > 50°$. [b] Temperature determined from measurements of the cell constants of a standard crystal of glycine. [c] Using carbon tetrachloride and hexane. [d] Data reduction and corrections performed with use of the program KAPPA, part of the CRYSNET system at Brookhaven National Laboratory. [e] Absorption correction computed with use of ABSOR, part of the CRYSNET system at Brookhaven National Laboratory.

Determination and Refinement of the Structure. E statistics indicated a centrosymmetric structure, and therefore a Patterson map[18] was calculated and solved in the centric space group $P\bar{1}$. (Subsequent attempts to refine the structure in the acentric space group $P1$ did not give satisfactory results.) After several cycles of refinement,[19]

(7) Wells, C. F.; Fox, D. *J. Chem. Soc., Dalton Trans.* **1977**, 1498, 1502.
(8) Brown, J. K.; Fox, D.; Heyward, M. P.; Wells, C. F. *J. Chem. Soc., Dalton Trans.* **1979**, 735.
(9) Fox, D.; Wells, C. F. *J. Chem. Soc., Faraday Trans. 1* **1982**, *78*, 1525, 2929.
(10) Macartney, D. H.; Sutin, N. *Inorg. Chim. Acta* **1983**, *74*, 221.
(11) Macartney, D. H.; Sutin, N. *Inorg. Chem.* **1983**, *22*, 3530.
(12) McAuley, A.; Macartney, D. H.; Oswald, T. *J. Chem. Soc., Chem. Commun.* **1982**, 274. Macartney, D. H.; McAuley, A. *Can. J. Chem.* **1983**, *61*, 103.
(13) Murray, C. K.; Margerum, D. W. *Inorg. Chem.* **1983**, *22*, 463.
(14) Brodovitch, J. C.; Haines, R. I.; McAuley, A. *Can. J. Chem.* **1981**, *59*, 1610.
(15) "International Tables for X-ray Crystallography", 3rd ed.; Kynoch Press: Birmingham, England, 1969; Vol. I: (a) p 74; (b) p 75.
(16) Raston, C. L.; White, A. H. *J. Chem. Soc., Dalton Trans.* **1976**, 7.
(17) Churchill, M. R.; Kalra, K. L. *Inorg. Chem.* **1974**, *13*, 1427.
(18) Except where otherwise noted, all calculations were performed by using SHELX-76: Sheldrick, G. M. In "Computing in Crystallography"; Schenck, H., Olthof-Hazekamp, R., van Koningveld, H., Bassi, G. C., Eds.; Delft University Press: Delft, Holland, 1978; pp 34–42.
(19) Neutral-atom scattering factors and anomalous dispersion corrections were taken from: "International Tables for X-ray Crystallography"; Kynoch Press: Birmingham, England, 1974; Vol. IV, pp 99, 149.

Table II. $Ni(bpy)_3(ClO_4)_3 \cdot 2CH_3CN \cdot 0.5CH_2Cl_2$ Atomic Coordinates[a,b]

atom	x	y	z
Ni	0.25482 (9)	0.20938 (6)	0.40873 (10)
Cl1	0.12934 (15)	0.19424 (9)	0.89314 (15)
O11	0.2517 (5)	0.2283 (3)	0.9772 (5)
O12	0.0661 (5)	0.2490 (3)	0.8119 (5)
O13	0.1424 (5)	0.1296 (3)	0.8051 (5)
O14	0.0553 (5)	0.1686 (3)	0.9767 (5)
Cl2	0.64733 (15)	0.14705 (11)	0.16158 (17)
O21	0.6248 (5)	0.1286 (3)	0.2829 (5)
O22	0.7685 (6)	0.1862 (6)	0.1940 (9)
O23	0.5592 (6)	0.1949 (4)	0.1015 (5)
O24	0.6283 (9)	0.0777 (4)	0.0712 (8)
Cl3	0.70250 (19)	0.43926 (12)	−0.0426 (3)
O31	0.6184 (5)	0.4920 (3)	−0.0866 (5)
O32	0.6656 (8)	0.3900 (6)	0.0347 (9)
O33	0.8221 (7)	0.4761 (5)	0.0102 (13)
O34	0.6938 (13)	0.3874 (6)	0.8359 (14)
N1	0.1577 (5)	0.2753 (3)	0.2820 (5)
C12	0.2322 (6)	0.3218 (4)	0.2320 (6)
C13	0.1831 (7)	0.3717 (4)	0.1433 (7)
C14	0.0526 (7)	0.3755 (4)	0.1072 (7)
C15	−0.0195 (7)	0.3281 (4)	0.1600 (7)
C16	0.0334 (6)	0.2790 (4)	0.2439 (6)
N2	0.3962 (5)	0.2642 (3)	0.3737 (5)
C22	0.3667 (6)	0.3137 (4)	0.2831 (6)
C23	0.4609 (7)	0.3541 (4)	0.2424 (7)
C24	0.5843 (6)	0.3438 (4)	0.3007 (7)
C25	0.6135 (6)	0.2949 (4)	0.3975 (7)
C26	0.5163 (6)	0.2549 (4)	0.4311 (7)
N3	0.2328 (4)	0.1251 (3)	0.2583 (5)
C32	0.1322 (5)	0.0712 (3)	0.2458 (6)
C33	0.1089 (6)	0.0043 (4)	0.1564 (6)
C34	0.1840 (6)	−0.0063 (4)	0.0767 (7)
C35	0.2865 (6)	0.0501 (4)	0.0890 (6)
C36	0.3054 (6)	0.1148 (4)	0.1808 (6)
N4	0.1050 (5)	0.1538 (3)	0.4251 (5)
C42	0.0585 (5)	0.0895 (3)	0.3353 (6)
C43	−0.0503 (6)	0.0465 (4)	0.3354 (7)
C44	−0.1126 (6)	0.0700 (5)	0.4270 (7)
C45	−0.0634 (6)	0.1348 (5)	0.5161 (7)
C46	0.0460 (6)	0.1750 (4)	0.5137 (6)
N5	0.3544 (5)	0.1482 (4)	0.5468 (5)
C52	0.3807 (6)	0.1834 (6)	0.6766 (7)
C53	0.4291 (7)	0.1393 (8)	0.7830 (7)
C54	0.4449 (8)	0.0626 (7)	0.7582 (10)
C55	0.4196 (7)	0.0310 (6)	0.6262 (9)
C56	0.3753 (6)	0.0739 (5)	0.5254 (7)
N6	0.2847 (6)	0.2860 (4)	0.5743 (6)
C62	0.3548 (7)	0.2615 (5)	0.6893 (7)
C63	0.3934 (8)	0.3088 (7)	0.8080 (8)
C64	0.3643 (9)	0.3792 (8)	0.8124 (9)
C65	0.2900 (10)	0.4067 (6)	0.6933 (11)
C66	0.2525 (8)	0.3568 (5)	0.5754 (8)
N7	−0.3070 (6)	0.1220 (5)	0.6405 (7)
C71	−0.2765 (6)	0.1639 (5)	0.7345 (8)
C72	−0.2354 (8)	0.2159 (5)	0.8595 (9)
N8	−0.0523 (18)	0.3894 (20)	0.4814 (18)
C81	−0.0583 (14)	0.3927 (17)	0.591 (3)
C82	−0.0309 (16)	0.4205 (9)	0.7303 (16)
N8A	−0.0638 (16)	0.3413 (10)	0.539 (4)
Cl81	−0.147 (3)	0.4196 (20)	0.718 (4)
Cl82	0.016 (3)	0.5073 (12)	0.616 (2)
Cl41	−0.4416 (8)	0.4852 (3)	0.5521 (7)
Cl42	−0.6988 (6)	0.5111 (3)	0.4285 (5)
C4	−0.544 (4)	0.542 (2)	0.433 (4)

[a] Numbers in parentheses are errors in the last significant digit(s). [b] The site occupancy factor is 0.89 for C(82), 0.54 for N(8), 0.35 for N(8A), 0.11 for Cl(81) and Cl(82), and 0.39 for Cl(41), Cl(42), and C(4). For all other atoms it is 1.00.

it was observed that one of the acetonitriles and the dichloromethane were disordered. The disordered acetonitrile was determined to consist of at least two partial acetonitriles and one partial dichloromethane sharing the same volume with one atom common to all three molecules. The site occupation factor of the atoms in the disordered solvent molecules were allowed to refine with use of a common factor for each

Table III. Bond Distances (Å) and Angles (deg) for $Ni(bpy)_3^{3+}$

	Nickel–Ligand Distances		
Ni–N(1)	1.995 (5)	Ni–N(4)	1.924 (6)
Ni–N(2)	1.924 (5)	Ni–N(5)	2.020 (6)
Ni–N(3)	2.006 (5)	Ni–N(6)	2.023 (6)
	Nickel–Ligand Angles		
N(1)–Ni–N(2)	82.8 (1)	N(2)–Ni–N(6)	88.6 (2)
N(1)–Ni–N(3)	91.3 (2)	N(3)–Ni–N(4)	83.1 (2)
N(1)–Ni–N(4)	93.0 (2)	N(3)–Ni–N(5)	92.4 (2)
N(1)–Ni–N(5)	176.3 (2)	N(3)–Ni–N(6)	173.7 (2)
N(1)–Ni–N(6)	94.9 (2)	N(4)–Ni–N(5)	87.4 (2)
N(2)–Ni–N(3)	93.1 (2)	N(4)–Ni–N(6)	95.5 (3)
N(2)–Ni–N(4)	174.4 (2)	N(5)–Ni–N(6)	81.4 (2)
N(2)–Ni–N(5)	97.0 (2)		

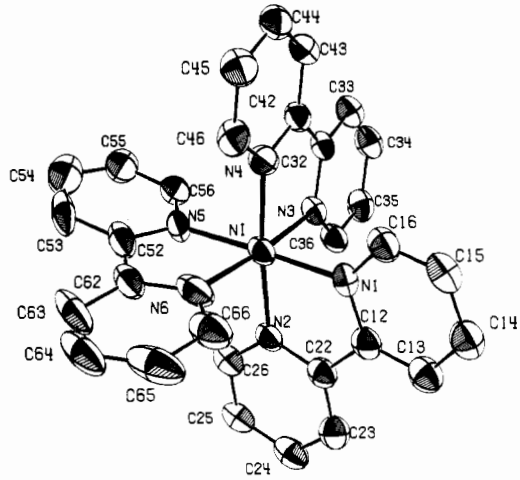

Figure 1. ORTEP drawing of the $Ni(bpy)_3^{3+}$ cation with thermal ellipsoids at the 50% probability level. N(1), N(3), N(5), and N(6) form the equatorial plane with N(2) and N(4) in the axial positions. The atom-numbering scheme used is shown.

member of a group. The formula calculated from the density of the crystal is $Ni(C_{10}H_8N_2)_3(ClO_4)_3 \cdot 2CH_3CN \cdot 0.5CH_2Cl_2$, so that it is likely that an acetonitrile also shares the site occupied by the dichloromethane near the inversion center at ($^1/_2$, $^1/_2$, $^1/_2$). It, however, could not be found.

Anisotropic temperature factors were used for all the non-hydrogen atoms except for the carbon of the dichloromethane near ($^1/_2$, $^1/_2$, $^1/_2$), which had a fixed isotropic temperature factor. The location of the hydrogen atoms on the bipyridine ligands and on the ordered acetonitrile were calculated (C–H bond length 0.95 Å). The hydrogen atoms were allowed to "ride"[18] on the atom to which they were attached. A common isotropic temperature factor for all the bipyridine hydrogen atoms refined to $U = 0.065$ (5) Å^2 and to $U = 0.10$ (2) Å^2 for the hydrogen atom on the acetonitrile. The hydrogen atoms on the disordered solvent molecules were not located.

The quantity $\sum w(|F_o| - |F_c|)^2$, where $w = 2.2962/(\sigma(F_o)^2 + 0.006F_o^2)$ was minimized in the least-squares refinement. During the final complete cycle the largest parameter shift was less than 0.06 of its error. The final R_1 value[20] was 0.096. The final weighted discrepancy index R_2[20] was 0.132. A final difference Fourier map revealed two peaks of about 1.6 and 1.4 e/Å^3 (less than one-third the size of a carbon atom) near the nickel and peaks of less than 1 e/Å^3 near the chloride atoms of the perchlorate ions.

The final non-hydrogen atomic positions are reported in Table II. The Ni–N distance and N–Ni–N angles with their standard deviations are presented in Table III. The thermal parameters for the non-hydrogen atoms and the positional parameters for the hydrogen atoms are presented in Tables S1 and S2, respectively. The interatomic distances and angles for the bipyridine rings, the anions, and the solvent molecules are listed in Table S3. A listing of the final observed and calculated structure factor amplitudes can be found in Table S4, and the hydrogen bonds and other close contacts are presented in Table S5.

(20) $R_1 = \sum||F_o| - |F_c||/\sum|F_o|$; $R_2 = [\sum w(|F_o| - |F_c|)^2/\sum w|F_o|^2]^{1/2}$.

Table IV. Structural Data for Some Polypyridine and Related Complexes[a]

complex		M-L, Å		ref
		equatorial	axial	
$Ni(bpy)_3^{3+}$	$(\pi d)^6(d_{x^2-y^2})^1$	2.022 (6), 2.000 (5)	1.924 (6)	this work
$Ni(bpy)_3^{2+}$	$(\pi d)^6(d_{x^2-y^2})^1(d_{z^2})^1$	2.089 (9)	2.089 (9)	23
NiL^{2+}	$(\pi d)^6(d_{z^2})^2$	1.959 (2)		32
$Ni(Cl)_2L$	$(\pi d)^6(d_{x^2-y^2})^1(d_{z^2})^1$	2.102 (3), 2.060 (3)	2.562 (1)	32
$Co(terpy)_2^{2+}$ [b]	$(\pi d)^6(d_{x^2-y^2})^1$	2.083 (4),[c] 2.104 (5)[d]	1.921 (5),[c] 1.942 (7)[d]	31
$Co(terpy)_2^{2+}$ [e]	$(\pi d)^5(d_{x^2-y^2})^1(d_{z^2})^1$	2.136 (5)	2.028 (6)	30
$Ni(Cl)_2L'^{+}$	$(\pi d)^6(d_{z^2})^1$	1.970 (4)	2.452 (4)	34
$Ni(Cl)_2L'$	$(\pi d)^6(d_{x^2-y^2})^1(d_{z^2})^1$	2.058 (8)	2.492 (3)	35
$Ni(F)_2L$	$(\pi d)^6(d_{x^2-y^2})^1(d_{z^2})^1$	2.090 (6)	2.087 (7)	33
$Ni(H_2PO_4)_2L''^{+}$	$(\pi d)^6(d_{x^2-y^2})^1$	2.013 (3), 1.993 (3)	2.061 (3)	36

[a] Abbreviations used: L = 5,5,7,12,12,14-hexamethyl-1,4,8,11-tetraazacyclotetradecane; L' = 1,4,8,11-tetraazacyclotetradecane; L'' = 5,7,7,12,14,14-hexamethyl-1,4,8,11-tetraazacyclotetradecane. [b] Iodide salt. [c] Low temperature, $\mu_{eff} = 2.2\ \mu_B$. [d] Room temperature, $\mu_{eff} = 3.2\ \mu_B$. [e] Perchlorate salt.

Results and Discussion

Description of the Structure. A view of the $Ni(C_{10}H_8N_2)_3^{3+}$ ion and the atom-labeling scheme used are shown in Figure 1. The six nitrogen atoms of the three 2,2'-bipyridine ligands form a tetragonally distorted octahedron about the Ni^{3+} center. The six Ni–N bonds form three sets so that two of the six Ni–N bonds are 2.022 (6) Å, two are 2.000 (5) Å, and two are 1.924 (6) Å. The four longer bonds form the equatorial plane while the two shorter bonds are in the axial positions. The short axial bonds result in a decrease of 0.02 Å in the Ni–N bond lengths for the other pyridine of the bipyridine ligand. The third bipyridine ligand has two equal Ni–N bond lengths. The Ni(III) complex thus exhibits a Jahn–Teller distortion, with the axial Ni–N bonds 0.1 Å shorter than the equatorial bonds. The Jahn-Teller distortion is expected[21] for low-spin Ni^{3+} in an octahedral environment. The average Ni–N bond length of 1.982 (46) Å determined here agrees with the value of 1.98 Å found by EXAFS studies.[22] Two values have been reported for the average Ni–N bond length in $Ni(bpy)_3^{2+}$: 2.089 (4)[23a] and 2.107 (15) Å.[23b] The former value is in good agreement with the Ni–N distance in $Ni(phen)_3^{2+}$ (2.090 Å).[23c] With use of this value the axial and equatorial bonds in $Ni(bpy)_3^{3+}$ are 0.17 and 0.08 Å shorter, respectively, than in the corresponding Ni(II) complex.

The bond lengths and angles within the bipyridine ligands (average intrapyridine C–C bond length 1.38 (3) Å, average bridging C–C' bond length 1.452 (2) Å, average C–N bond length 1.35 (2) Å, Table III) are similar to those found in other structures.[3] The only significant deviations are in the bond lengths involving C(64). The C(64)–C(63) bond length of 1.312 (18) Å is short, and the C(64)–C(65) bond length of 1.440 (14) Å is long. This part of the ring appears to be slightly disordered due to the disorder in the neighboring solvent system. The angles between the pyridine rings in the bipyridine ligands are 4.4, 6.4, and 12.7°, similar to those found in $[Ni(bpy)_3]SO_4$.[23a] All the pyridine rings are planar with the maximum deviation of an atom from the least-squares plane being 0.02 Å. The Ni^{3+} lies in the equatorial plane with the longest deviation from this plane being 0.01 Å.

The average bond distance in each of the three perchlorate anions is 1.442 (6), 1.416 (19), and 1.40 (5) Å and the average bond angle is 109.5 (7), 109 (2), and 109 (5)° for the perchlorates centered around Cl(1), Cl(2), and Cl(3) respectively.

Table V. Rate Constants for Electron-Exchange Reactions of Polypyridine Complexes at 25 °C

couple	configns	Δd_0, Å	k_{ex},[a] $M^{-1}\ s^{-1}$	ref
$Ni(bpy)_3^{3+/2+}$	$(\pi d)^6(\sigma d)^1/(\pi d)^6(\sigma d)^2$	0.12	2×10^3 (1.0)	*b*, 11
$Co(terpy)_2^{3+/2+}$	$(\pi d)^6/(\pi d)^6(\sigma d)^1$	0.13	3×10^3 (0.1)	*b*, 41–44
$Co(bpy)_3^{3+/2+}$	$(\pi d)^6/(\pi d)^5(\sigma d)^2$	0.19	18 (0.1)	3, 6, *c*
$Co(bpy)_3^{2+/+}$	$(\pi d)^5(\sigma d)^2/(\pi d)^6(\sigma d)^2$	−0.02	1×10^9 (0.5)	3
$Fe(bpy)_3^{3+/2+}$	$(\pi d)^5/(\pi d)^6$	0.00	3×10^8 (5.5)	6, *d*
$Ru(bpy)_3^{3+/2+}$	$(\pi d)^5/(\pi d)^6$	0.00[e]	4×10^8 (0.1)	*f*

[a] Ionic strength (M) given in parentheses. [b] This work. [c] H. M. Newmann, quoted in ref 41. [d] Ruff, I.; Zimonyi, M. *Electrochim. Acta* 1973, *18*, 515. [e] Difference in the metal–nitrogen distances assumed to be the same as in the corresponding iron(II)–iron(III) couple. [f] Young, R. C.; Keene, F. R.; Meyer, T. J. *J. Am. Chem. Soc.* 1977, *99*, 2468.

Crystal Packing. The crystal is held together by a series of C–H···O hydrogen-bond[3,24] and other C–H···O interactions (Table S5). These interactions involve the hydrogens on the bipyridine ligands and on the acetonitrile of crystallization. The disordering of some of the solvent molecules results in a partial disordering of one of the perchlorate ions and part of one of the bipyridine ligands. A Cl(3)–Cl(81) contact of 3.42 Å, which is too short for a Cl–Cl contact,[25] and a Cl(81)–O(34) contact of 2.508 Å indicate that the perchlorate ion centered around Cl(3) must be in a different position ~11% of the time (when the dichloromethane including Cl(81) is present). This disordering, although too small to be clearly seen, is reflected in the higher standard deviations in the bond lengths and bond angles and in the larger thermal ellipsoids associated with the atoms in these groups.

Comparisons with Other Structures. In common with $Ni(bpy)_3^{3+}$, tris(2,2'-bipyridine)copper(II) diperchlorate[26] also exhibits a Jahn–Teller distortion. In the latter case an unequal increase in the axial Cu–N bond lengths to 2.226 (7) and 2.450 (7) Å vs. 2.031 (6) Å for the average equatorial Cu–N bond length is observed. The increase in the axial bond lengths is normal for a d^9 copper(II) complex and can be attributed to the presence of two electrons in the d_{z^2} orbital. In the nickel(III) complex the opposite type of Jahn–Teller distortion is observed: the axial bonds are *shorter* than the equatorial bonds. This can be explained by the single unpaired electron in nickel(III) being in the $d_{x^2-y^2}$ rather than in the d_{z^2} orbital. This interpretation is consistent with ESR studies on $Ni(bpy)_3^{3+}$: for this complex $g_\parallel = 2.026$ and $g_\perp = 2.137$, with

(21) Cotton, F. A.; Wilkinson, G. "Advanced Inorganic Chemistry", 4th ed.; Wiley: New York, 1980.
(22) Brunschwig, B. S., unpublished observations.
(23) (a) Wada, A.; Sakabe, N.; Tanaka, J. *Acta Crystallogr., Sect. B: Struct. Crystallogr. Cryst. Chem.* **1976**, *B32*, 1121. (b) Wada, A.; Katayama, C.; Tanaka, J. *Ibid.* **1976**, *B32*, 3194. (c) Frenz, B. A.; Ibers, J. A. *Inorg. Chem.* **1972**, 11, 1109. (d) Finney, A. J.; Hitchman, M. A.; Kepert, D. L.; Raston, C. L.; Rowbottom, G. L.; White, A. H. *Aust. J. Chem.* **1981**, 34, 2177.
(24) Hamilton, W. C.; Ibers, J. A. "Hydrogen Bonding in Solids"; W. A. Benjamin: New York, 1968.
(25) Pauling, L. "The Nature of the Chemical Bond"; Cornell University Press: Itaca, NY, 1960; p 259.
(26) Anderson, O. P. *J. Chem. Soc., Dalton Trans.* **1972**, 2597.

the $g_{\parallel}$ feature split into a quintet due to interactions with the two equivalent axial nitrogen atoms.[27] The four equatorial nitrogens give rise to a hyperfine multiplet splitting of the $g_{\perp}$ component of the spectrum. A similar tetragonal distortion is observed in $Cu(terpy)_2^{2+}$ (terpy = 2,2′:6,2″-terpyridine).[28,29] In this complex the Cu–N distance for the central (axial) pyridines is decreased to 1.98 Å while the Cu–N distance for the distal (equatorial) pyridines is increased to 2.18 Å.

A comparison can also be made with the structures of high-spin[30] and low-spin[31] $Co(terpy)_2^{2+}$ (Table V). In these structures decreases of 0.06 and 0.11 Å in the equatorial and axial bond lengths respectively (Table V) are observed on going from high-spin $[(\pi d)^5(\sigma d)^2]$ to a low-spin $[(\pi d)^6(\sigma d)^1]$ cobalt(II) center. A decrease similar in magnitude to those seen in the axial bond lengths in $Co(terpy)_2^{2+}$ is also seen in the equatorial bond lengths (as well as a large increase in the axial bond lengths) on going from six-coordinate high-spin[32] $Ni(Cl)_2L$ (Table V) to four-coordinate low-spin[32] NiL^{2+}. The equatorial bond lengths in $Ni(Cl)_2L$ are unequal (2.102 (3) and 2.060 (3) Å) probably due to steric factors. If the average equatorial Ni–N bond length of 2.090 (6) Å found in $Ni(F)_2L$[33] (in which the steric factors are less important) is used, a decrease of 0.13 Å is observed in the equatorial bond lengths on going from a high-spin six-coordinate to a low-spin four-coordinate metal center. In each case a bond length increase of 0.13–0.14 Å is observed upon addition of an electron to the appropriate σd orbital. Similar considerations can account for most of the decrease of 0.08 Å in the equatorial bond lengths and 0.17 Å in the axial bond lengths observed in this study on going from high-spin $[(\pi d)^6(\sigma d)^2]$ $Ni(bpy)_3^{2+}$[23] to low-spin $[(\pi d)^6(\sigma d)^1]$ $Ni(bpy)_3^{3+}$. In the latter case it is also necessary to allow for a small bond length decrease (~0.04 Å[6]) expected when the charge of the metal center is increased from 2+ to 3+ (all other factors remaining the same).

The structures of *trans*-dichloro(1,4,8,11-tetraazacyclotetradecane)nickel(III) perchlorate, $[Ni([14]aneN_4)(Cl)_2]ClO_4$,[34] and of the corresponding nickel(II) complex[35] have also been determined. Upon oxidation to the nickel(III) complex, the equatorial Ni–N bond length decreases from 2.058 (8) to 1.970 (4) Å and the axial Ni–Cl bond length decreases from 2.492 (3) to 2.452 (4) Å. The decrease in the equatorial bond length of 0.088 Å is similar to the decrease of 0.08 Å observed in the present study, but the decrease in the axial Ni–Cl bond length of only 0.040 Å is significantly less than the 0.17 Å observed here. This can be understood if in the macrocyclic system the transferred electron is in a $d_{x^2-y^2}$ orbital: this could result in the axial bond lengths showing simply the decrease of 0.04 Å expected for the increase in charge on the metal center, while steric effects prevent the Ni–N bond lengths in the macrocycle from showing a larger decrease upon oxidation. This interpretation implies that the unpaired electron in the nickel(III) macrocycle is in a d_{z^2} orbital, a result that is consistent with EPR studies of nickel(III) oligopeptides.[36]

The structure of another octahedral nickel(III) complex, *trans*-bis(dihydrogen phosphato)(*meso*-5,7,7,12,14,14-hexamethyl-1,4,8,11-tetraazacyclotetradecane)nickel(III) perchlorate, $[Ni(meso\text{-}Me_6[14]aneN_4)(H_2PO_4)_2]ClO_4$, has been reported,[37] but the corresponding nickel(II) structure has not been determined, so a direct comparison of the structures cannot be made. Nevertheless, the Ni–(OPO_3H_2) axial bond length observed in this complex is almost identical with the value of 2.060 (10) Å found for equatorially coordinated $PO_4H_2^-$ in $NiNa_2H_8(PO_4)_4{\cdot}4H_2O$.[38]

$Ni(bpy)_3^{3+}/Ni(bpy)_3^{2+}$ Electron-Exchange Barriers. Next we discuss the $Ni(bpy)_3^{3+/2+}$ electron-exchange rate in terms of the configuration changes accompanying the electron transfer and compare the $Ni(bpy)_3^{3+/2+}$ system with other polypyridine couples. As mentioned in the Introduction, the exchange rate variations for the polypyridine couples are expected to reflect primarily changes in the nuclear factor and specifically in the inner-shell reorganization energy. The latter is given by

$$\Delta G^*_{in} = \tfrac{1}{2}\sum f_i((\Delta d_0)_i/2)^2 \qquad (4)$$

where f_i is the reduced force constant for the ith inner-sphere vibration and is defined in terms of the normal mode force constants for that vibration, $f_i = 2f_{ox}f_{red}/(f_{ox} + f_{red})$, $(\Delta d_0)_i$ is the bond length difference for bond i in the two oxidation states, $(\Delta d_0)_i = (d_{red} - d_{ox})_i$, and the sum is taken over all the intramolecular vibrations. The "average" value of Δd_0 for the nickel–nitrogen bonds in the $Ni(bpy)_3^{3+/2+}$ system calculated from eq 5 is 0.12 (1) Å. The exchange rate for the Ni-

$$\Delta d_0 = \{[2(\Delta d_0)_{ax}^2 + 4(\Delta d_0)_{eq}^2]/6\}^{1/2} \qquad (5)$$

$(bpy)_3^{3+/2+}$ couple has been estimated to be 2×10^3 M^{-1} s^{-1} at 25 °C and 1.0 M ionic strength.[11] The $Co(terpy)_2^{3+/2+}$ electron exchange also involves the transfer of a dσ electron between low-spin (d^6 and d^7) configurations.[39–42] A self-exchange rate constant of 3×10^3 M^{-1} s^{-1} (μ = 0.10 M) has been calculated for this couple from cross-reaction data.[41,43] The structure of the $Co(terpy)_2^{3+}$ cation has recently been determined:[44] the distal Co–N distances are 1.921 (7)–1.937 (7) Å, and the central Co–N distances are 1.863 (7)–1.853 (7) Å. The average Co–N bond distance (1.91 Å) may be compared with the values for low-spin $Co(bpy)_3^{3+}$ (1.93 (2) Å)[45] and $Co(phen)_3^{3+}$ (1.91 (1) Å).[6] When low-spin $Co(terpy)_2^{2+}$ (Table IV) is oxidized to $Co(terpy)_2^{3+}$, the axial (central) Co–N distances decrease 0.06 Å (as expected for the change in the charge on the metal) while the equatorial (distal) Co–N distances decrease 0.15 Å as a result of the removal of an electron from the antibonding $d_{x^2-y^2}$ orbital. The average value (eq 5) of Δd_0 for the cobalt–nitrogen bonds in $Co(terpy)_2^{3+/2+}$ is 0.13 Å, similar to the average Δd_0 for the $Ni(bpy)_3^{3+/2+}$ couple.

In Table V the metal–ligand bond distance differences and exchange rates for the $Ni(bpy)_3^{3+/2+}$ and $Co(terpy)_2^{3+/2+}$ systems are compared with those found for other bipyridine couples. As discussed previously,[6] Δd_0 is expected to be small

(27) Brodovitch, J. C.; Haines, R. I.; McAuley, A. *Can. J. Chem.* **1981**, *59*, 1610.
(28) Allman, R.; Henke, U.; Reinen, D. *Inorg. Chem.* **1978**, *17*, 378.
(29) Arriortua, M. I.; Rojo, T.; Amigo, J. M.; Germain, G.; Declerrq, J. P. *Acta Crystallogr., Sect. B: Struct. Crystallogr. Cryst. Chem.* **1982**, *B38*, 1323.
(30) Figgis, B. N.; Kucharski, E. S.; White, A. H. *Aust. J. Chem.* **1983**, *36*, 1537.
(31) Figgis, B. N.; Kucharski, E. S.; White, A. H. *Aust. J. Chem.* **1983**, *36*, 1527.
(32) Ito, T.; Toriumi, K. *Acta Crystallogr., Sect. B: Struct. Crystallogr. Cryst. Chem.* **1981**, *B37*, 88.
(33) Toriumi, K.; Ito, T. *Acta Crystallogr., Sect. B: Struct. Crystallogr. Cryst. Chem.* **1981**, *B37*, 240.
(34) Ito, T.; Sugimoto, M.; Toriumi, K.; Ito, H. *Chem. Lett.* **1981**, 1477.
(35) Bosnich, B.; Mason, R.; Pauling, P. J.; Robertson, G. B.; Tobe, M. L. *J. Chem. Soc., Chem. Commun.* **1965**, 97.
(36) Lappin, A. G.; Murray, C. K.; Margerum, D. W. *Inorg. Chem.* **1978**, *17*, 1630.
(37) Zeigerson, E.; Bar, I.; Bernstein, J.; Kirschenbaum, L. J.; Meyerstein, D. *Inorg. Chem.* **1982**, *21*, 73.
(38) Boudjada, P. A.; Durif, A.; Guitel, J. C. *Acta Crystallogr., Sect. B: Struct. Crystallogr. Cryst. Chem.* **1978**, *B34*, 17.
(39) ESR and magnetic susceptibility studies[40,42] show the $Co(terpy)_2^{2+}$ ion to be predominantly low spin in solution at room temperature.
(40) J. Lewis, quoted in ref 41.
(41) Farina, R.; Wilkins, R. G. *Inorg. Chem.* **1968**, *7*, 514.
(42) Kremer, S.; Henke, W.; Reinen, D. *Inorg. Chem.* **1982**, *21*, 3013.
(43) Cummins, D.; Gray, H. B. *J. Am. Chem. Soc.* **1977**, *99*, 5158.
(44) Figgis, B. N.; Kucharski, E. S.; White, A. H. *Aust. J. Chem.* **1983**, *36*, 1563.
(45) Yanagi, K.; Ohashi, Y.; Sasada, Y.; Kaizu, Y.; Kobayashi, H. *Bull. Chem. Soc. Jpn.* **1981**, *54*, 118.

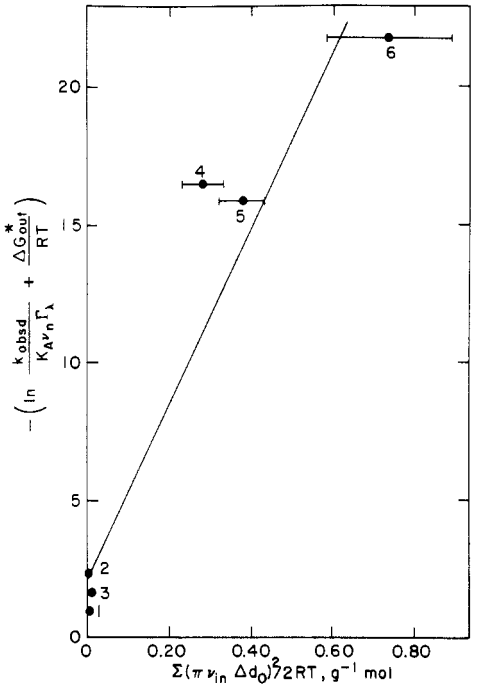

Figure 2. Plot of $-[\ln (k_{obsd}/K_A\nu_n\Gamma_\lambda) + \Delta G^*_{out}/RT]$ against $\sum_i[\pi\nu_{in}^2(\Delta d_0)]_i/2RT$ for exchange reactions of metal polypyridine complexes at 25 °C: (1) $Ru(bpy)_3^{3+/2+}$; (2) $Fe(bpy)_3^{3+/2+}$; (3) $Co(bpy)_3^{2+/+}$; (4) $Ni(bpy)_3^{3+/2+}$; (5) $Co(terpy)_2^{3+/2+}$; (6) $Co(bpy)_3^{3+/2+}$.

when there is no difference in the $d\sigma$ populations of the oxidized and reduced forms of the couple. Consistent with this, the oxidized and reduced forms of $Co(bpy)_3^{2+/+}$, $Fe(bpy)_3^{3+/2+}$, and $Ru(bpy)_3^{3+/2+}$ have the same $d\sigma$ population and Δd_0 for the couples is very small; on the other hand, the oxidized and reduced forms of $Ni(bpy)_3^{3+/2+}$ and $Co(bpy)_3^{3+/2+}$ differ by one and two $d\sigma$ electrons, respectively, and Δd_0 is 0.12 Å for the nickel couple and 0.19 Å for the cobalt couple. Although this model is crude, and must be used with caution, it evidently does account for the Δd_0 trends seen in the polypyridine systems.[46]

We next consider the relation between the exchange rate constants and Δd_0. In Figure 2[47] values of the logarithm of the rate constant for the exchange divided by the stability constant of the precursor complex, the frequency factor, and the nuclear tunneling factor, plus the outer-sphere barrier divided by RT, are plotted as a function of $\Sigma[\pi\nu_{in}^2 \times (\Delta d_0)]_i^2/2RT$, where ν_{in} is the reduced frequency[48,49] for a particular metal–ligand vibration in the two oxidation states ($\nu_{in} = [2\nu_{red}^2\nu_{ox}^2/(\nu_{red}^2 + \nu_{ox}^2)]^{1/2}$). For the $Ni(bpy)_3^{3+/2+}$ and $Co(terpy)_2^{3+/2+}$ couples, in which Jahn–Teller tetragonal distortions are observed in the low-spin Ni(III) and Co(II) species, the quantity $[\nu_{in}(\Delta d_0)]^2$ was determined for each axis and was then summed over all the metal–ligand vibrations (of eq 5). The intercept of the line in Figure 2 is the average value of κ_{el} for the series: for the present purpose the intercept was taken as 2.2, the value implicated in a more extensive correlation that included aquo and ammine complexes.[6] The slope of the line is equal to the effective mass of a pyridine ring of the polypyridine ligand: the line in Figure 2 corresponds to an effective mass of 32. Although there is considerable uncertainty in the slope and the estimate of the effective mass must be regarded as tentative at this time, an effective mass of this magnitude (which corresponds roughly to the mass of an imine group) seems reasonable since it would be expected to be less than the mass of a rigid pyridine but greater than that of the coordinated nitrogen.[50]

With the exception of the $Ni(bpy)_3^{3+/2+}$ couple, the points in Figure 2 are reasonably close to the line drawn through the data. The direction of the deviation of the $Ni(bpy)_3^{3+/2+}$ couple is such as to imply a larger nonadiabaticity for the $Ni(bpy)_3^{3+/2+}$ exchange. In the $Ru(bpy)_3^{3+/2+}$ exchange the delocalization of metal $d\pi$ density onto the π^* orbitals of the ligand allows for electron exchange via ligand π^*–π^* overlap, resulting in $\kappa_{el} \approx 1$. If, however, the exchange in this couple required direct 4d–4d overlap, the process would be highly nonadiabatic[51] at the separation distance defined by the first contact of the bpy ligands. The mixing of $d\sigma$ and $L\pi^*$ orbitals in the $Ni(bpy)_3^{3+/2+}$ couple is presumably less efficient than the mixing of the $d\pi$ and $L\pi^*$ oribtals in the $Ru(bpy)_3^{3+/2+}$, $Fe(bpy)_3^{3+/2+}$, and $Co(bpy)_3^{2+/+}$ systems, consistent with a larger nonadiabaticity for the $Ni(bpy)_3^{3+/2+}$ exchange. It is, nevertheless, surprising that a lower κ_{el} value is implicated for the $Ni(bpy)_3^{3+/2+}$ than for the $Co(bpy)_3^{3+/2+}$ exchange: the electronic coupling in these systems is enhanced by mixing of excited-state with ground-state wave functions,[52] and a larger adiabaticity for the cobalt system would imply more efficient mixing in the cobalt system, despite the fact that the cobalt exchange is formally spin forbidden. Indeed the "spin-forbidden" $Co(bpy)_3^{3+/2+}$ exchange does not seem to be inherently less adiabatic than the "spin-allowed" $Co(terpy)_3^{3+/2+}$ exchange: the difference in the exchange rates of the two cobalt couples can be adequately accounted for in terms of their Δd_0 differences. Further comparisons of the reactivity of these systems as well as refinement of the model used are obviously of considerable interest.

The above discussion neglects any contribution to ΔG^*_{in} from differences in the intraligand bond distances and angles in the two oxidation states. Such differences appear to be negligible for the $M(bpy)_3^{3+/2+}$ couples considered here. On the other hand, the ligands in $Co(bpy)_3^+$ have some bpy^- character, which is essentially absent in $Co(bpy)_3^{2+}$; it has been estimated[3] that the resulting difference in intraligand distances may contribute 3 ± 1 kcal mol^{-1} to ΔG^*_{in}. Including this intraligand contribution to the activation barrier will, of course, lower the calculated rate constant for the $Co(bpy)_3^{2+/+}$ exchange; this lowering is, however, largely compensated for by the higher frequency of the intraligand modes (which results in a higher effective nuclear frequency), and this effect has not been included here.

The above discussion has shown that the structural results for the tris(bipyridine)nickel complexes, when employed in the semiclassical outer-sphere electron-transfer model, provide a satisfactory rationalization of the moderate self-exchange rate constant for the $Ni(bpy)_3^{3+/2+}$ couple. In addition, the overall trends seen are consistent with the results found for other metal

(46) When there is a departure from octahedral symmetry (as in the case of $Ni(bpy)_3^{3+}$ and, for example, macrocyclic complexes), the Δd_0 values along the particular axes (Table IV) can be correlated with changes in the $d_{x^2-y^2}$ and d_{z^2} populations, as discussed earlier.

(47) The following parameters were used in Figure 2 [(data point) K_A in M^{-1}, ln ν_n, ln Γ_λ]: (1) 0.83, 27.6, 0; (2) 0.33, 27.6, 0; (3) 0.83, 29.2, 0; (4) 0.63, 29.7, 0.5; (5) 0.63, 29.8, 0.8; (6) 0.33, 29.8, 1.6.

(48) Hutchinson, B.; Takemoto, J.; Nakamoto, K. *J. Am. Chem. Soc.* **1970**, *92*, 3335. Saito, Y.; Takemoto, J.; Hutchinson, B.; Nakamoto, K. *Inorg. Chem.* **1972**, *11*, 2003.

(49) The $Ni(bpy)_3^{3+}$ Ni–N stretching frequencies observed in this study at 375 and 275 cm^{-1} are assigned to the shorter axial and longer equatorial bonds, respectively. Similarly, for $Co(terpy)_2^{2+}$, peaks observed at 430 and 250 cm^{-1} are assigned to stretching vibrations of the central and distal Co–N bonds, respectively.

(50) In some previous applications[3,4,6] the inner-shell reorganization energy for the $Co(bpy)_3^{3+/2+}$ exchange had been calculated with use of a reduced force constant of 1.69×10^5 dyn cm^{-1}, the value of the reduced Co–NH_3 force constant in the $Co(NH_3)_6^{3+/2+}$ couple. The reduced force constant calculated with the effective mass of a bpy/2 equal to 32 is 1.76×10^5 dyn cm^{-1}, in gratifying agreement with the force constant assumed earlier.

(51) Sutin, N.; Brunschwig, B. S. *ACS Symp. Ser.* **1982**, *No. 198*, 105.

(52) Mok, C. Y.; Zanella, A.; Creutz, C.; Sutin, N. *Inorg. Chem.* **1984**, *23*, 2891.

tris(polypyridine) couples. Additional structural and vibrational studies, leading to refinements in metal–ligand and intraligand distances, angles, and force constants, might result in further improvements in the agreement between observed and calculated exchange rates, especially for systems in which there is considerable intraligand reorganization and in which a large nonadiabaticity is implicated.

Acknowledgment. We wish to acknowledge very helpful discussions with Drs. Carol Creutz and Bruce Brunschwig and experimental assistance from P. Mulligan (Queens University, Kingston, Ontario, Canada). This work was performed at Brookhaven National Laboratory under contract with the U.S. Department of Energy and supported by its Office of Basic Energy Sciences. D.H.M. wishes to thank the Natural Sciences and Engineering Research Council of Canada for support in the form of a Postdoctoral Fellowship.

Registry No. $Ni(bpy)_3(ClO_4)_3 \cdot 2CH_3CN \cdot 0.5CH_2Cl_2$, 92127-01-0.

Supplementary Material Available: Thermal parameters for the non-hydrogen atoms (Table S1), atomic coordinates for the hydrogen atoms (Table S2), bond distances and angles for the bipyridine rings, the anions, and the solvent molecules (Table S3), observed and calculated structure factors (Table S4), and hydrogen bonds and other close contacts (Table S5) (28 pages). Ordering information is given on any current masthead page.

Contribution from the Institut für Anorganische Chemie, Universität Bern, CH-3000 Bern 9, Switzerland

Transfer of Electronic Excitation Energy in the Antiferromagnets $RbMnCl_3$, $CsMnCl_3$, $CsMnBr_3$, and Rb_2MnCl_4

URSULA KAMBLI† and HANS U. GÜDEL*

Received December 12, 1983

Transfer of electronic excitation energy was studied in crystals of the antiferromagnetic compounds $RbMnCl_3$, $CsMnCl_3$, $CsMnBr_3$, and Rb_2MnCl_4. Nominally pure as well as Er^{3+}- and Nd^{3+}-doped samples were studied by time-resolved luminescence spectroscopy. Both host and guest emissions were followed as a function of concentration, temperature, and time delay after the excitation pulse. There is multiple evidence for excitation transfer. The corresponding rates were quantitatively determined and rationalized in terms of a kinetic model. The transfer to traps is thermally activated, and the activation energies for the four compounds are 537, 1259, 508, and 38 cm^{-1}, respectively. The activation energies are correlated to spectroscopically determined electronic splittings of the $^4T_1$ state. They can be rationalized in terms of a purely excitonic intrasublattice mechanism for long-range energy transfer. No correlation could be established between the energy-transfer characteristics and the dimensionality of the crystal lattice.

1. Introduction

Excitation energy transfer (ET) is a well-known phenomenon in condensed Mn^{2+} compounds. MnF_2[1] as well as the alkali metal fluoromanganates(II) $KMnF_3$, $RbMnF_3$,[2] and $CsMnF_3$[3] have been studied extensively with this respect. ET is very efficient in these compounds down to 4.2 K. As a consequence, there is hardly any intrinsic emission. Most of the emission observed is from Mn^{2+} traps, i.e. Mn^{2+} ions that are slightly perturbed by adjacent impurities such as Ca^{2+}, Zn^{2+}, and Mg^{2+} [4] or by crystal imperfections. Efficient ET at room temperature was also reported for the quasi-1-D antiferromagnets TMMC,[5] $CsMnBr_3$,[6] and $CsMnCl_3 \cdot 2H_2O$,[7] as well as for the alkali metal chloromanganates(II) $CsMnCl_3$[8], $RbMnCl_3$,[8] $KMnCl_3$,[9] and $NaMnCl_3$.[10] In contrast to the fluoride compounds, however, energy transfer is negligible at 4.2 K and the luminescence in these compounds is essentially intrinsic at low temperatures. In the compounds $CsMnCl_3 \cdot 2H_2O$, $RbMnCl_3$, and $CsMnCl_3$, in which fine structure was resolved on the high-energy side of the luminescence band, no trap emission from perturbed Mn^{2+} sites was detected.[11,8]

Energy transfer in the chloromanganates(II) and $CsMnBr_3$ is strongly temperature dependent and becomes efficient only above 50 K. The two-dimensional (2-D) antiferromagnet Rb_2MnCl_4 represents an intermediate case.[12] At 4.2 K ET is not completely absent, but it is not as effective as in MnF_2.

Electronic d–d transitions within the Mn^{2+} ions are spin and parity forbidden. The most likely mechanism for excitation transfer is therefore an exchange mechanism.[13] Exchange interactions in the ground state are responsible for the magnetic properties. A consequence of the exchange coupling in the ground state is the antiferromagnetic order. Exchange pathways depend on structural parameters like bond distances and bridging geometries. Magnetic properties are therefore strongly related to crystal structures. Accordingly, the linear-chain compounds TMMC, $CsMnBr_3$, and $CsMnCl_3 \cdot 2H_2O$ behave as quasi-1-D antiferromagnets, and the layer-structured Rb_2MnCl_4 behaves as a quasi-2-D antiferromagnet.[14–17]

A similar structural dependence is expected for the exchange

† Present address: Institute of Applied Physics, University of Bern, 3012 Bern, Switzerland.

(1) Wilson, B. A.; Yen, W. M.; Hegarty, J.; Imbusch, G. F. *Phys. Rev. B: Condens. Matter* **1979**, *19*, 4238.
(2) (a) Strauss, E.; Gerhardt, V.; Riederer, H. *J. Lumin.* **1976**, *12/13*, 239. (b) Iverson, M. V.; Sibley, W. A. *Phys. Rev. B: Condens. Matter* **1980**, *21*, 2522 and references therein.
(3) Moncorgé, R.; Jacquier, B.; Madej, C.; Blanchard, M.; Brunel, L. C. *J. Phys. (Orsay, Fr.)* **1982**, *43*, 1267.
(4) Greene, R. L.; Sell, D. D.; Feigelson, R. S.; Imbusch, G. F.; Guggenheim, H. J. *Phys. Rev.* **1968**, *171*, 600.
(5) Yamamoto, H.; McClure, D. S.; Marzzacco, C.; Waldman, M. *Chem. Phys.* **1977**, *22*, 79.
(6) McPherson, G. L.; Francis, A. H. *Phys. Rev. Lett.* **1978**, *41*, 1681.
(7) McPherson, G. L.; Willard, S. C. *Chem. Phys. Lett.* **1981**, *78*, 135.
(8) Kambli, U.; Güdel, H. U. *J. Phys. C* **1984**, *17*, 4041.
(9) McPherson, G. L.; Devaney, K. O.; Willard, S. C.; Francis, A. H. *Chem. Phys. Lett.* **1979**, *68*, 9.
(10) Matyushkin, E. V.; Eremenko, V. V.; Bron, R. Y. *J. Magn. Magn. Mater.* **1980**, *15–18*, 1043.
(11) Jia, W.; Strauss, E.; Yen, W. M. *Phys. Rev. B: Condens. Matter* **1981**, *23*, 6075.
(12) Kambli, U.; Güdel, H. U.; Briat, B. *J. Phys. C* **1984**, *17*, 3113.
(13) Dexter, D. L. *J. Chem. Phys.* **1953**, *21*, 836.
(14) Dingle, R.; Lines, M. E.; Holt, S. L. *Phys. Rev.* **1969**, *187*, 643.
(15) Eibschütz, M.; Sherwood, R. C.; Hsu, F. S. L.; Cox, D. E. *AIP Conf. Proc.* **1972**, *No. 10*, 684.
(16) Kobayashi, H.; Tsujikawa, I.; Friedberg, S. A. *J. Low Temp. Phys.* **1973**, *10*, 621.
(17) Witteveen, H. T. *J. Solid State Chem.* **1974**, *11*, 245.

0020-1669/84/1323-3479$01.50/0